Earth and Planetary Science Letters 515 (2019) 13–25

Contents lists available at ScienceDirect

Earth and Planetary Science Letters

www.elsevier.com/locate/epsl

The rise of pinnacle reefs: A step change in marine evolution triggered by perturbation of the global carbon cycle

Patrick I. McLaughlin [a], Poul Emsbo [b], Carlton E. Brett [c], Alyssa M. Bancroft [a], André Desrochers [d], Thijs R.A. Vandenbroucke [e]

[a] Indiana Geological and Water Survey, Indiana University, Bloomington, Indiana 47405, USA
[b] U.S. Geological Survey, Denver Federal Center, Denver, Colorado 80225, USA
[c] Department of Geology, University of Cincinnati, Cincinnati, Ohio 45221, USA
[d] Department of Earth and Environmental Sciences, University of Ottawa, Ottawa, Ontario K1N 6N5, Canada
[e] Department of Geology, Ghent University, Ghent, Belgium

ARTICLE INFO

Article history:
Received 25 September 2018
Received in revised form 23 February 2019
Accepted 28 February 2019
Available online 25 March 2019
Editor: D. Vance

Keywords:
Silurian
chronostratigraphy
carbon isotope excursion
chemostratigraphy
carbonates
sequence stratigraphy

ABSTRACT

The first appearance of pinnacle reef tracts, composed of hundreds to thousands of localized biogenic structures protruding tens to hundreds of meters above the surrounding mid-Silurian seafloor, represents a step change in the evolution of the marine biosphere. This change in seafloor morphology opened a host of new ecological niches that served as "evolutionary cradles" for organism diversification. However, the exact timing and drivers of this event remain poorly understood. These uncertainties remain, in large part, due to a paucity of index fossils in the reef facies, the difficulty of correlating between the offshore pinnacle reefs and more temporally well-constrained shallow marine facies, and cryptic unconformities that separate amalgamated reefs. Here we use $\delta^{13}C_{carb}$ stratigraphy within a sequence stratigraphic framework to unravel these complex relationships and constrain the origination of Silurian pinnacle reef tracts in the North American midcontinent to near the *Pt. celloni* Superzone—*Pt. am. amorphognathoides* Zonal Group boundary of the mid-Telychian Stage.

In addition, we identify a striking relationship between pulses of reef development and changes in global $\delta^{13}C_{carb}$ values and sea level. Viewed through this new perspective, we correlate prolific periods of reef development with short-lived carbon isotope ($\delta^{13}C_{carb}$) excursions and eustatic sea level change that, ultimately, reflect perturbations to the global carbon cycle. From changes in the dominance of microbial reefs of the Cambrian to metazoan colonization of reefs in the Middle Ordovician, through the subsequent collapse of metazoan diversity with the Late Ordovician mass extinction, and the first appearance of early Silurian (Llandovery) pinnacle reef tracts and their proliferation during the late Silurian (Wenlock-Pridoli) and Devonian, major reef formation intervals increasingly coincide with $\delta^{13}C_{carb}$ excursions. These patterns suggest that Paleozoic reef evolution was the product of environmental forcing by perturbations of the global carbon cycle.

1. Introduction

For the last 540 million years, reefs have served as a wellspring for the diversification of marine organisms. The appearance of vertically tiered and cryptic habitats created by the development of reefs on otherwise featureless seafloors provided nuclei for biodiversification (Kiessling et al., 2010). The evolution of this geomorphological and ecological phenomenon is described as one of the most significant events in the history of life (Flügel and Kiessling, 2002). Microbial reefs produced by cyanobacteria, the precursors of metazoan reefs, first appeared in the Archean (James and Wood, 2010; Riding, 2011). With the exception of ecological niche expansion from supratidal to shelf margin settings, early reef characteristics remained unchanged for billions of years, typically forming only gentle swells dotting the Proterozoic seafloor. Metazoan colonization of microbial reefs began in the latest Neoproterozoic to early Cambrian. Despite this change, reefs remained low-relief features that hosted relatively low-diversity populations. The late Cambrian to Early Ordovician featured a resurgence of microbially dominated reefs (Riding, 2006). The protracted Great Ordovician Biodiversification Event (Early to Middle Ordovician) that followed marked a profound change in reef development. It fostered high-relief stromatactis-bearing mud mounds and the evolution of di-

E-mail address: pimclaug@iu.edu (P.I. McLaughlin).

https://doi.org/10.1016/j.epsl.2019.02.039

verse metazoan reef assemblages including, for the first time, a consortium of corals, sponges, and bryozoans (Webby, 2002) that acted as important framework builders and sediment bafflers. Yet it was not until the emergence of large wave- and current-resistant pinnacle reef tracts during the early Silurian that the seascapes of planet Earth forever changed and altered the trajectory of marine biodiversity (Kiessling, 2002).

The dominance of pinnacle reefs (defined here as localized biogenic marine structures with >10 m of original synoptic relief) through the Silurian and Devonian has long been hypothesized as a consequence of a prolonged period of stable high-CO_2 greenhouse conditions (Copper, 2002). However, recent sedimentologic and oxygen isotopic data indicate this interval was marked by pulses of severe cooling and glaciation, generally interpreted as reflecting the drawdown of atmospheric CO_2 during perturbations to the global carbon cycle (e.g., Trotter et al., 2016). Thus, the relationship between high-CO_2 greenhouse climatic states and periods of reef dominance merits re-evaluation. Viewed at a coarse temporal scale, the Silurian, Devonian, Jurassic, and Miocene are intervals of the Phanerozoic having elevated abundances of pinnacle reefs (Kiessling, 2002). However, when viewed at a finer temporal resolution, these intervals are characterized by short-lived "reef episodes" separated by longer intervals of muted reef development (e.g., Brunton et al., 1998; Webby, 2002). Consequently, reef evolution may not be gradualistic, but instead characterized by abrupt changes in abundance, size, composition, and spatial distribution.

The primary objective of this study is to couple high-resolution facies analysis and $\delta^{13}C_{carb}$ stratigraphy within a sequence stratigraphic framework to refine the age assessment and constrain the environmental conditions of the first Silurian pinnacle reef tracts—features that were hundreds to thousands of kilometers long and composed of thousands of individual reefs with an intercontinental distribution that reflects a fundamental change of global seascapes. A derivative outcome of this investigation is the recognition of a relationship between periods of reef development, sea level fluctuation, and global $\delta^{13}C_{carb}$ variations. Specifically, this empirical relationship indicates that periods of reef proliferation correspond in part with $\delta^{13}C_{carb}$ excursions throughout much of the Paleozoic. We use the observed correlation to explore cause-and-effect relationships between global carbon cycle perturbations and the environmental changes that promoted pinnacle reef formation.

1.1. $\delta^{13}C_{carb}$ stratigraphy

Advances made over the last several decades in high-resolution carbon isotope stratigraphy now enable global deep-time stratigraphic correlation at an unprecedented resolution and are enhancing the study of ancient coupled marine and atmospheric processes (e.g., Jenkyns et al., 1994; Kaljo et al., 1997; Gill et al., 2011). Carbon isotope stratigraphy of carbonate ($\delta^{13}C_{carb}$), in particular, applied in unison with other biostratigraphic, chemostratigraphic, geochronologic, and astrochronologic data, has revolutionized our ability to precisely constrain the age of strata. Recent Silurian studies (Fig. 1; e.g., Cramer et al., 2010, 2012) are at the forefront of this research, demonstrating that some intervals can now be globally correlated at a precision approaching 100 k.y. or better. The Silurian global composite chronostratigraphic standard (*sensu* Cramer et al., 2011), together with more recent biostratigraphic and chemostratigraphic studies of Silurian strata in eastern North America (e.g., McLaughlin et al., 2012; Waid and Cramer, 2017), provide the framework for chronostratigraphic interpretation employed in this study (Fig. 2).

Multiple studies now demonstrate Silurian $\delta^{13}C_{carb}$ excursions are coincident with evidence of global bioevents and oceanic and climatic changes (Munnecke et al., 2010). Recognition that modern carbonate platforms have sediment $\delta^{13}C_{carb}$ values that are decoupled from ocean dissolved inorganic carbon (DIC) reservoirs suggests caution is necessary when using $\delta^{13}C_{carb}$ values from marine carbonates, particularly from epeiric seas, to interpret global processes (see detailed discussion in Supplementary Text Section 1). Nonetheless, Silurian $\delta^{13}C_{carb}$ excursions are repeatedly shown to correspond with dramatic periods of global cooling and glaciation, sea-level fluctuation, increased primary productivity, redox changes, and globally correlated time-specific facies (Brett et al., 2012; Trotter et al., 2016; Emsbo, 2017). Surprisingly, these patterns are not unique to the Silurian. Similarly, coupled $\delta^{13}C_{carb}$ and environmental changes are well documented throughout the geologic column (Supplemental Text Section 1). A particularly instructive Paleozoic example, is the upper Cambrian (Ferungian) Steptoean Positive Carbon Isotope Excursion (SPICE) (Gill et al., 2011). The SPICE is marked by faunal extinction and oceanic anoxia that, in places, spread from the deep sea to nearshore environments. Substantial burial of organic matter is hypothesized to be responsible for the +4.0 to +6.0‰ positive shift in global $\delta^{13}C_{carb}$ values and was accompanied by global cooling and a rapid lowering of global sea level associated with development of the Sauk II-III sequence boundary (Runkel et al., 1998). Related directly to our study, this late Cambrian event also coincided with a global change in reef types (Lee et al., 2015).

1.2. Pinnacle reefs: a stratigraphic challenge

Pinnacle reefs form within carbonate banks and adjacent slopes that straddle the interface between shallow and deep marine systems, forming a complex mosaic of different deposit types. The morphology and location of reefs reflect a range of tectonic, oceanographic, and climatic processes (cf., Schlager, 2005). The mosaic of reef and interreef strata characterizing the transition from shallow to deeper environments is difficult to study. Reefs, for example, have a tendency to nucleate on sea floor highs associated with older reefs. Contacts between discrete reef generations can be cryptic, even in full mountainside outcrop exposures. Thus, accurately tracing beds or even bed bundles associated with reefs systems from ramp or shelf, to slope, and out into deeper water deposits can be fraught with uncertainty. These complications, combined with the paucity of index fossils in reef intervals is, in part, responsible for enduring uncertainty about their genesis, particularly among pinnacle reefs. Nonetheless, the fossil reef literature amply addresses temporally episodic occurrence (at the scale of 10^6 yr), tectonic/geomorphologic controls on spatial distribution, as well as diverse composition, taxonomic diversity, and reef morphology (e.g., Heckel, 1974).

Silurian reefs are commonly apportioned into different categories as a function of size, spatial distribution, and compositional diversity and complexity. Onshore-offshore gradients, with smaller patch reefs nearshore, larger closely spaced pinnacle reefs at the ramp or shelf edge, and the tallest pinnacle reefs just farther outboard, characterize Silurian reef complexes. The largest known Silurian pinnacle reef tract spans more than 2000 km along the margin of the Franklinian Basin of the Canadian Arctic Archipelago and Greenland, which in places is more than several hundred meters thick (Sønderholm and Harland, 1989). The remote setting of this spectacular reef tract has impeded its detailed biostratigraphic study. However, the complex morphology of these reefs indicates a history of expansion and contraction that was likely interrupted by episodic exposure and wasting. Such complexities are common to pinnacle reef tracts and indicate the need for applying integrated high-resolution chronostratigraphic techniques, including carbon isotope stratigraphy, to fully characterize their histories.

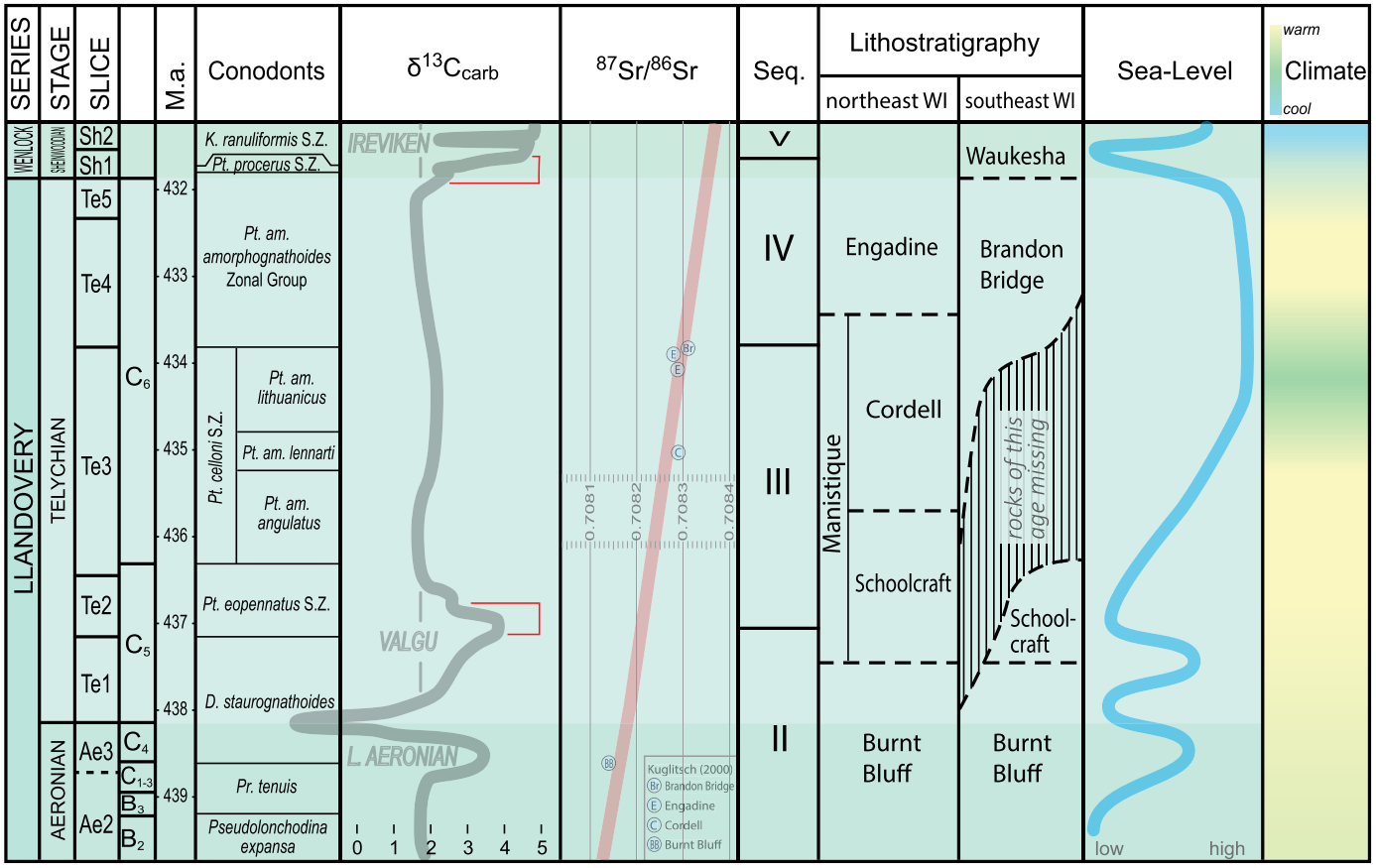

Fig. 1. Late Aeronian to early Sheinwoodian chronostratigraphic chart modified primarily from Cramer et al. (2011) with climatic interpretation from Trotter et al. (2016). See Supplemental Fig. 1 for more detail and full citations.

1.3. Silurian carbonates of the North American midcontinent

Silurian strata of the North American midcontinent region represent one of the world's great Phanerozoic carbonate factories (Kiessling et al., 2003). This region contains >1 million km^2 of a generally continuous, undeformed, shallow to deep marine carbonate record. The lower Silurian (Telychian) paleogeography of this region consists of a series of east-west-trending basins and arches that roughly paralleled the convergent southern Laurentian margin (Fig. 3C). The broad Algonquin Arch separated the Michigan Basin carbonate ramp from the mixed carbonates and clastics of the Appalachian Basin. The mid-Silurian chronostratigraphic framework for the Appalachian Basin and Algonquin Arch was recently revised by McLaughlin et al. (2012).

Reconstruction of mid-Silurian depositional history from the massive carbonate succession of the Michigan Basin has challenged generations of geologists. Regional chronostratigraphic correlation has been a challenge because, while most studies have consisted of detailed investigations, they were limited to discrete time intervals within this extensive carbonate system. For example, studies in northwestern Wisconsin (Door County, Fig. 3B) have generally focused on lower to middle Llandovery sections in relatively thin and scattered outcrop sections (see Harris and Waldhuetter, 1996 and references therein), whereas studies of southeastern Wisconsin have focused on younger Wenlock and Ludlow age strata in deep quarry exposures (cf., Watkins and McGee, 1994; Mikulic and Kluessendorf, 1998, and references therein). Regional correlation studies have largely pertained to the Llandovery brachiopod-bearing carbonate successions of Iowa and eastward across northern Wisconsin into the Upper Peninsula of Michigan and Ontario's Manitoulin Island (e.g., Colville and Johnson, 1982). The relative ages of strata across this region are largely defined by brachiopod lineages alone, thus complicating precise chronostratigraphic correlations derived from more cosmopolitan groups such as conodonts. However, recent work in the type-Llandovery area of Wales (Davies et al., 2016) and Iowa (Waid and Cramer, 2017) resulted in cross calibrations among brachiopods, conodonts, graptolites, chitinozoans, and the $\delta^{13}C_{carb}$ record (Fig. 1). Particularly relevant to our study is the occurrence of the *Pentamerus-Pentameroids* brachiopod lineage boundary at the Schoolcraft-Cordell contact (Johnson and Colville, 1982) in northeastern Wisconsin, indicating a lower Telychian age. Also important are the occurrence of zonally diagnostic conodonts *Pterospathodus eopennatus*, *Pterospathodus amorphognothoides amorphognothoides, Kockellela ranuliformis*, *Ozarkodina sagitta rhenana*, and *Kockellela walliseri* within the Brandon Bridge and Waukesha formations at Milwaukee (Kuglitsch, 2000; Kleffner et al., 2018), indicating a late Telychian to early Sheinwoodian age. These two robust chronostratigraphic tie points anchor our high-resolution $\delta^{13}C_{carb}$ analysis.

2. Study approach

Recent geologic mapping in eastern Wisconsin by the Wisconsin Geological and Natural History Survey generated more than a dozen new continuous drill cores spanning the entire Silurian record. These cores allow systematic evaluation of the Silurian strata in the less-studied subcrop belt of eastern Wisconsin. The Silurian succession comprises (in ascending stratigraphic order) the Burnt Bluff Group, Schoolcraft, Cordell, and Engadine formations in the northeast, and the Brandon Bridge and Waukesha formations in the southeast (Milwaukee area; Fig. 1). New and archived cores, totaling nearly 4 km of section, were carefully studied and

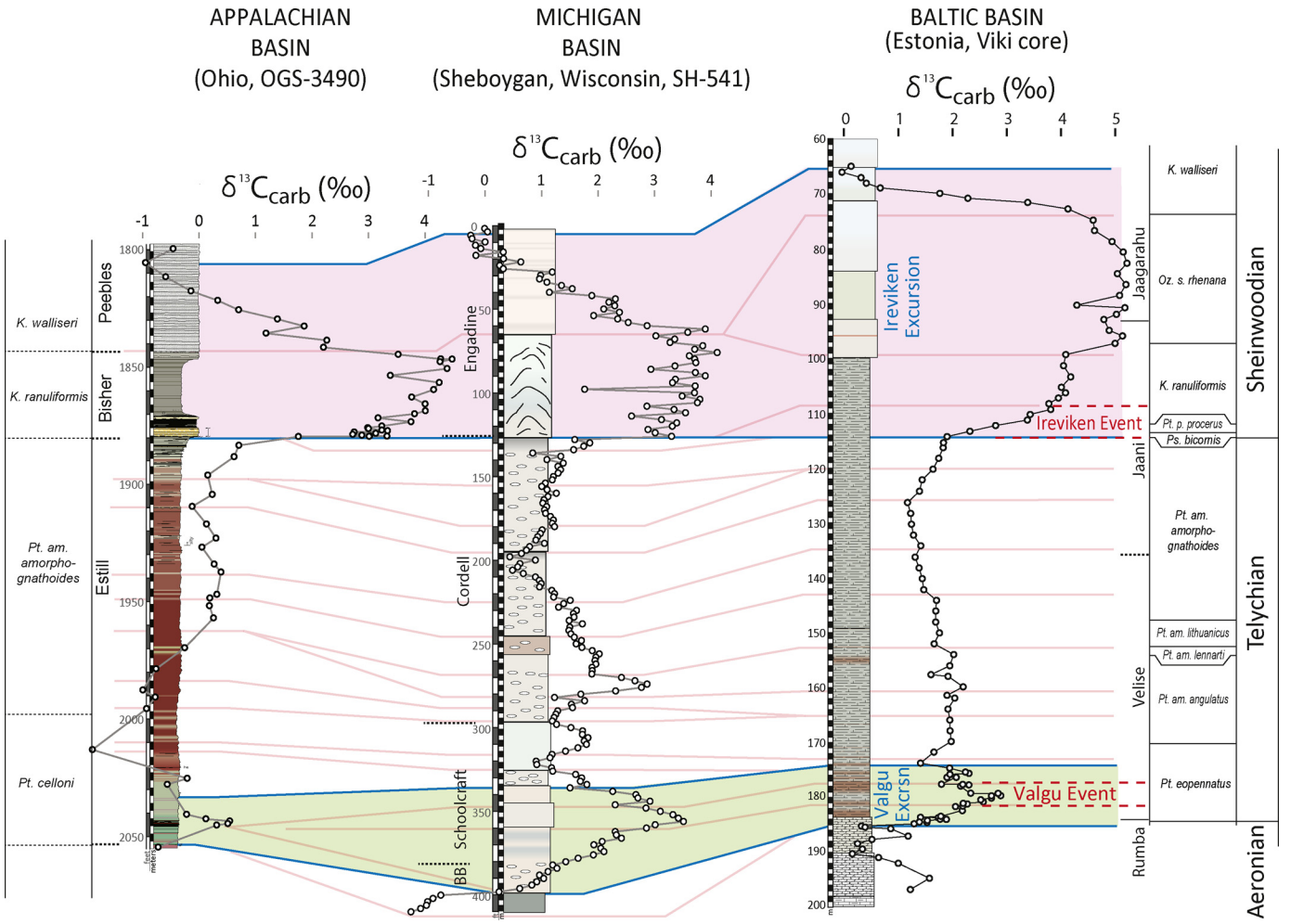

Fig. 2. Global chronostratigraphic correlation of the western Michigan Basin (eastern Wisconsin; Sheboygan core SH-541; data from McLaughlin et al., 2013) with sections from the Appalachian Basin (Ohio; McLaughlin et al., 2012) and Baltic Basin (Estonia; Kaljo et al., 2003); datum is base of the Ireviken Excursion.

provided comprehensive sampling across a broad range of facies. These strata were used to improve chronostratigraphic resolution and refine the paleogeographic setting and sea level history of deposits in the Wisconsin portion of the Michigan Basin at an unprecedented spatial and temporal scale (Fig. 3B).

Our detailed chronostratigraphic assessment of this carbonate succession integrates $\delta^{13}C_{carb}$ stratigraphy anchored by published conodont and brachiopod biostratigraphy, which thereby allows the use of data from both outcrops and subsurface cores across the region (Colville and Johnson, 1982; Kuglitsch, 2000). Moreover, conodont $^{87}Sr/^{86}Sr$ results (Kuglitsch, 2000) provide additional chronostratigraphic constraints for interpretation of our high-resolution $\delta^{13}C_{carb}$ profiles.

Whole-rock powders were typically collected from cores at 60 cm spacing, although spacing ranged from 5 to 120 cm depending on facies complexity. A total of 641 samples were preferentially drilled from micrite or associated fine-grained carbonate lithologies for carbon and oxygen isotope analysis. During sampling, brachiopods, corals, and other skeletal fragments were avoided where possible; vugs, stylolites, and similar metasomatic features were not sampled. Stable carbon and oxygen isotopes compositions were analyzed at the University of Kansas W.M. Keck Paleoenvironmental and Environmental Stable Isotope Laboratory and the Cornell University Stable Isotope Laboratory. Reproducibility of standards ranged from a standard deviation of 0.04 to 0.12‰.

Facies analysis of the study interval used a range of techniques. Cores were first photographed at high resolution under daylight spectrum light. Systematic comparative analysis of closely spaced cores enabled recognition of a range of lithologies, fabrics, fossil assemblages, fossil preservation, ichnofabrics, and trace fossil assemblages (Figs. 4–6; Supplemental Table 1; see McLaughlin et al., 2013, for additional details).

3. Results

Stratigraphic sections along the 200 km transect of the Michigan Basin produced $\delta^{13}C_{carb}$ profiles that share many features (Fig. 4). Values for $\delta^{13}C_{carb}$ range from −1.0 to +5.0‰, with well-stratified intervals (i.e., lacking reefs) displaying the lowest degree of scatter (see Supplemental Table 2 for raw data). Sequential samples generally define smooth trends and vary less than 0.2‰ between consecutive samples, except for occasional abrupt offsets that range from 0.3 to 2.0‰. The base of the upper Burnt Bluff Group is characterized by negative $\delta^{13}C_{carb}$ values that are about 1.1 to 2.1‰ below baseline of ~+1.0‰ (Fig. 4: Manitowoc, Sheboygan, and Oostburg sections). This negative feature, apparent in several of the analyzed sections, is overlain by at least three well-defined positive excursions. The lower positive excursion is characterized by a monotonic 5.0‰ rise from values near −1‰ at the base of the section (with occasional, minor, stepped offsets) upward through the Schoolcraft Formation, to a peak of +3.0 to +4.0‰. The end of the lower positive $\delta^{13}C_{carb}$ excursion is marked by an abrupt ~2.0‰ decrease coincident with the basal portion of the Cordell Formation. A minor positive inflection in $\delta^{13}C_{carb}$ val-

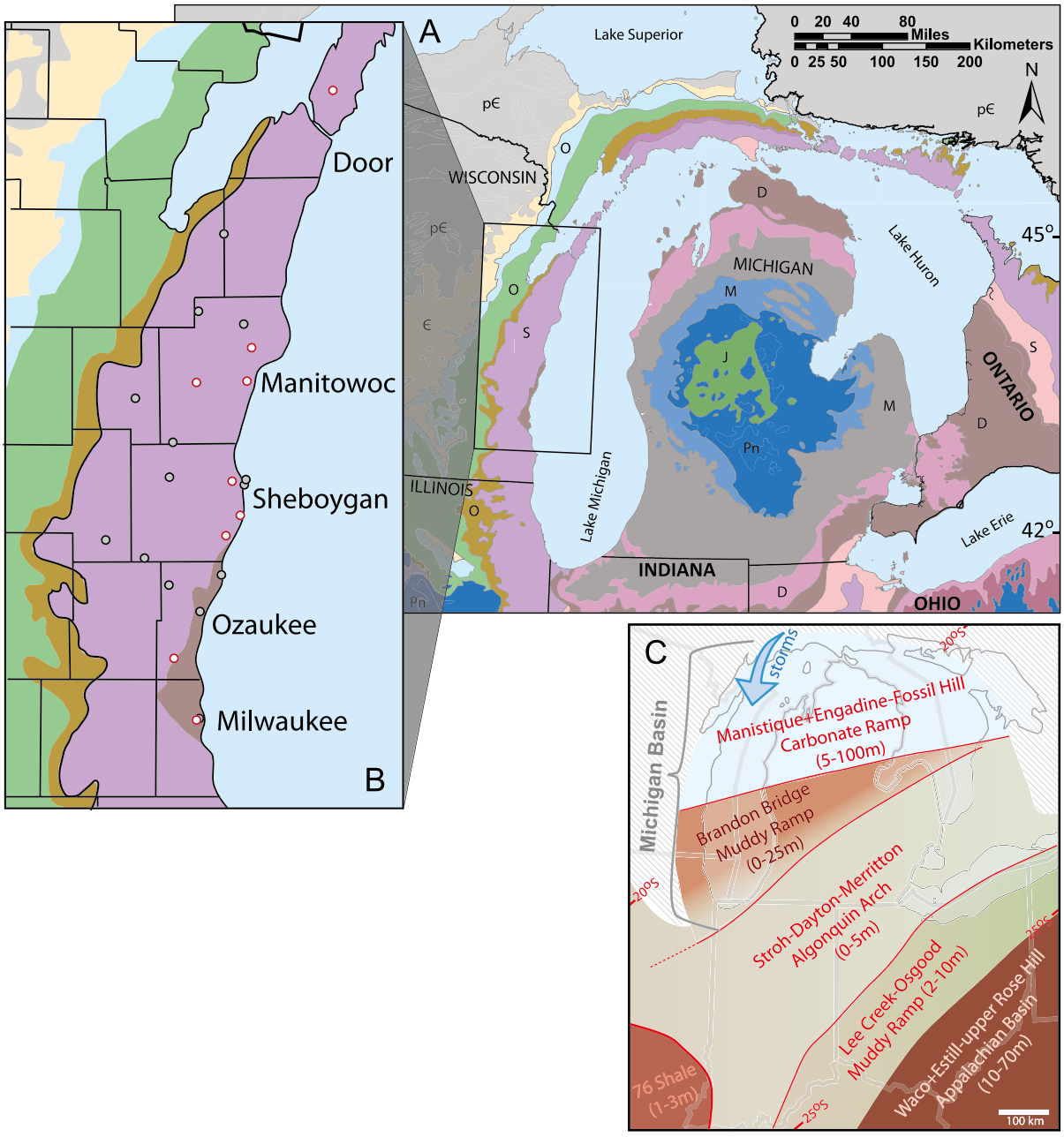

Fig. 3. Geologic setting. A. Simplified regional geologic map of the North American midcontinent. B. Inset map showing position of all Wisconsin cores studied (circles), with those shown in Fig. 4 in red. C. Generalized facies map for the Telychian of the midcontinent based on regional biostratigraphic correlation and lithofacies characterization of Rexroad (1980), Kuglitsch (2000), and McLaughlin et al. (2012). Thickness range of Telychian-age strata in parentheses; crosshatch indicates area of eroded Telychian strata. (For interpretation of the colors in the figure(s), the reader is referred to the web version of this article.)

ues (peaking near +3.0‰) occurs ~15 m above the lower $\delta^{13}C_{carb}$ excursion in sections north of Oostburg (SH-539). This positive $\delta^{13}C_{carb}$ excursion is unusual because it is not coincident with a facies change, but nonetheless, provides a useful marker for local correlation. A distinctive cluster of hardgrounds serves as the datum in Fig. 4. Above these hardgrounds, carbon isotope values shift to nearly +3.0‰ and define the second of the three major $\delta^{13}C_{carb}$ positive excursions. This excursion coincides with a shift to reef-associated facies in the Engadine Formation. The notable exception is the Sheboygan (SH-541) section near the center of the transect (Fig. 4) where the Engadine Formation reefs and the $\delta^{13}C_{carb}$ excursion above the hardgrounds pinch out. Notably, this section contains an upper tongue of the Cordell Formation that continues above the hardgrounds and is characterized by a distinctive $\delta^{13}C_{carb}$ profile having values gradually dropping to nearly 0.0‰, followed by a slight rise to values near +1.0‰ at the top of the unit. Importantly, the adjacent Manitowoc (MN-614) section contains a combination of these features, with the Engadine Formation reef facies and the middle $\delta^{13}C_{carb}$ excursion directly overlying the datum hardgrounds, followed by an abrupt transition into the upper tongue of the Cordell Formation. While the thickness of the upper Cordell in the Manitowoc section is only about half that in the Sheboygan core, $\delta^{13}C_{carb}$ profiles for strata derived from the two cores are similar. All stratigraphic sections north of Milwaukee, except the Jarmen Rd. section (truncated by the modern land surface), are capped by an upper tongue of the Engadine Formation whose $\delta^{13}C_{carb}$ values define the upper of the three positive excursions with values as high as +4.0 to +5.0‰.

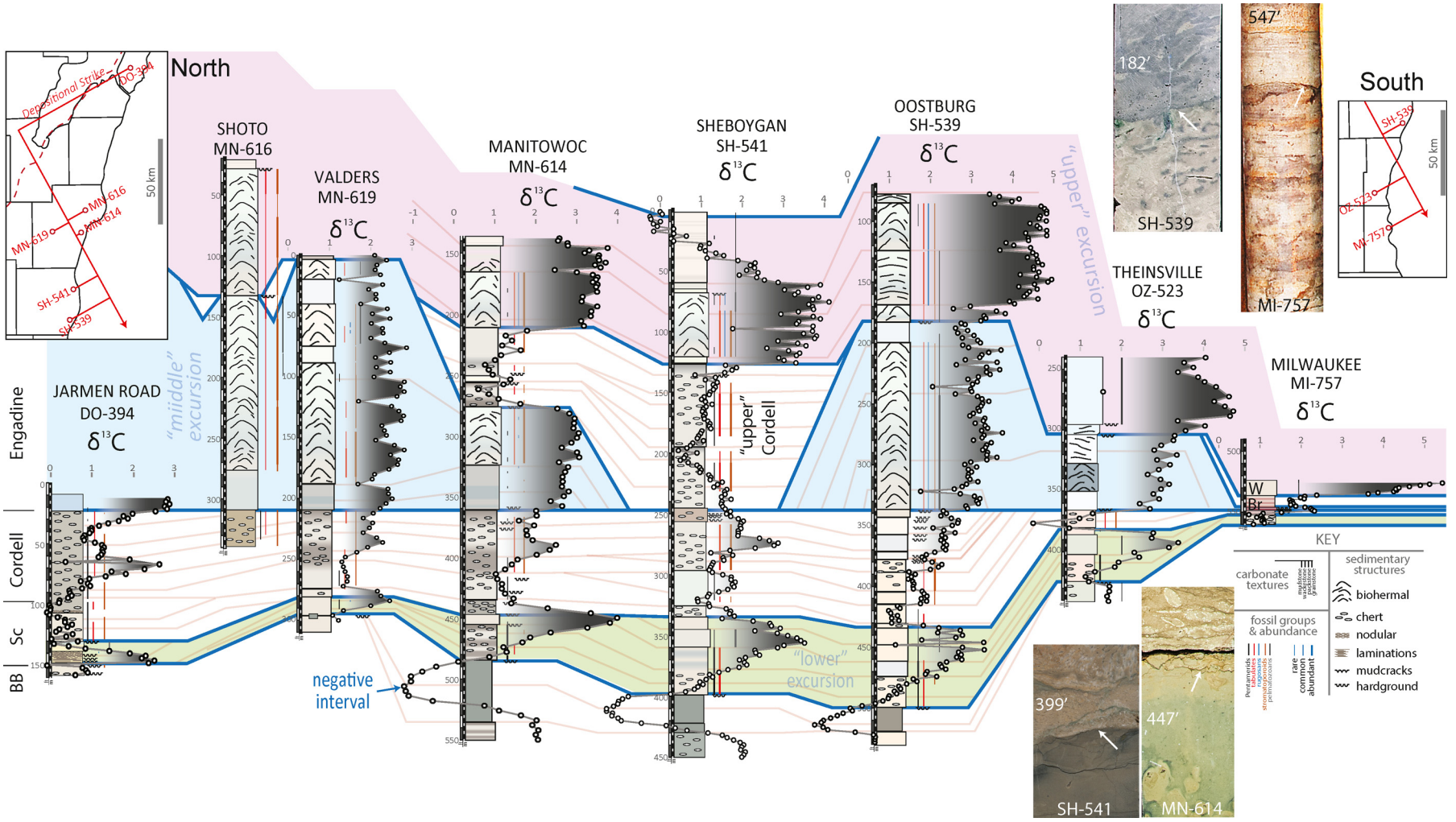

Fig. 4. Northwest-southeast $\delta^{13}C_{carb}$ and facies cross section from Door to Milwaukee Counties in Wisconsin, perpendicular to the inferred margin of the Michigan Basin (see arrow on inset maps). The sections (depth marked in feet) span the Burnt Bluff (BB), Schoolcraft (Sc), Cordell, and Engadine Formations in the north and the Brandon Bridge (Br) and overlying Waukesha (W) Formations in Milwaukee. The correlation datum is the top of a cluster of hardgrounds near the contact between the Cordell and Engadine formations and in the lower Brandon Bridge at Milwaukee. See key for lithologic symbols, grain size, and fossil abundance. Colors of lithologic logs approximate fresh rock color. Inset images show erosional contacts between facies packages from select localities (core number and depth labeled).

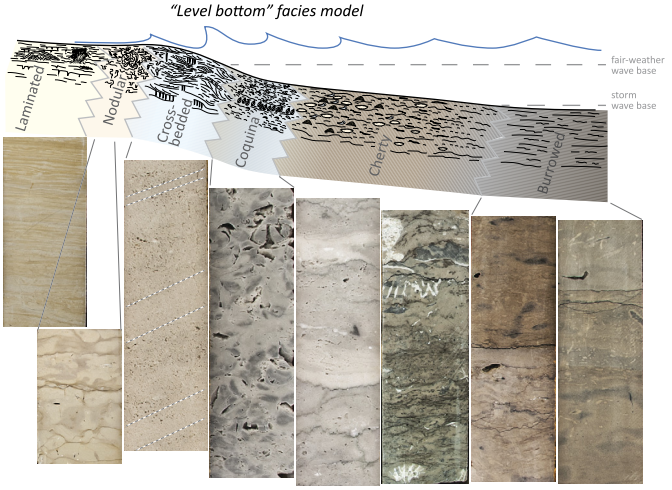

Fig. 5. Depositional model depicting relationship of facies (representative images of core for each) along an increasing water depth gradient (see Supplemental Table 1 for additional details).

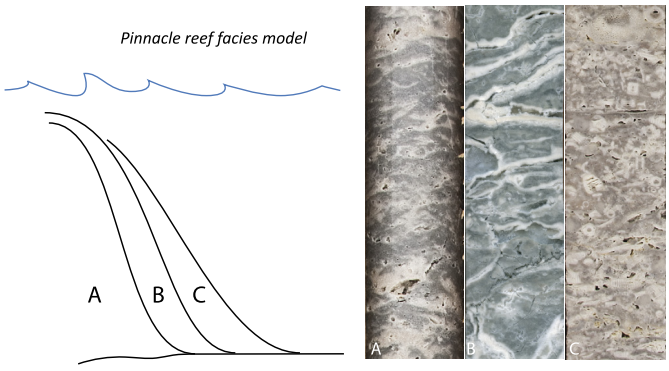

Fig. 6. Simplified facies model (and associated images) for pinnacle reefs in the study area. A) stromatactis core and flank facies. B) laminar stromatoporoid. C) crinoidal.

Importantly, the base of this upper positive excursion is marked by a sharp lithologic change and an abrupt increase in $\delta^{13}C_{carb}$ values. For example, where upper excursion reef facies overlie the Cordell Formation, values increase dramatically from +1.0 to >+4.0‰. Similarly, in sections where rocks of the upper excursion directly overlie the middle excursion reefs of the Engadine Formation, values jump from +3.0 to >+4.0‰ (see core photo of SH-539 at 182 ft, Fig. 4). In Milwaukee (MI-757) the interval is very different, with the Brandon Bridge Formation divided in half by the datum hardground cluster and sharply overlain by the Waukesha Formation containing the upper $\delta^{13}C_{carb}$ excursion (+4.0 to +5.0‰).

These complex spatial relationships, particularly between different tongues of the Cordell and Engadine formations, demonstrate the power of supplementing lithostratigraphy with $\delta^{13}C_{carb}$ stratigraphy to unravel the chronostratigraphy of reef sequences. For example, the stratigraphic relationships observed in Fig. 4 demonstrate that the upper tongue of the Cordell Formation above the hardground datum (preserved only in MN-614 and SH-541) is younger than the middle positive $\delta^{13}C_{carb}$ excursion. The sharp contact above the middle excursion reefs and the upper tongue of the Cordell Formation in MN-614 suggests an unconformable contact. Similarly, the sharp lithologic contact and offset in $\delta^{13}C_{carb}$ values at the base of the upper excursion suggest that it is separated from the underlying strata across the study area by an unconformity. These relationships provide strong evidence that the Engadine Formation is composed of a stacked sequence of discrete reef generations having two distinctly different ages.

Facies analysis was used to separate the lithostratigraphic units into six level-bottom categories that reflect deep subtidal to peritidal deposition (Fig. 5) and three biohermal facies (Fig. 6). In the study area, the stratigraphic distribution of facies is often compartmentalized; individual facies rarely grade into others, but rather are in sharp contact at occasionally mineralized hardground surfaces across which the facies change abruptly (Figs. 4 and 5). The subtidal "cherty" facies (Schoolcraft and Cordell formations) is one of the most distinct and common in the study area; less common are the "coquina" and "cross-bedded" facies (Schoolcraft and Engadine formations, respectively). Except for the coquina facies, deposits of each facies are dominated by micrite. The reefal facies (Engadine Formation; Fig. 6) exhibits thick muddy intervals that include abundant stromatactis that alternate with more fossiliferous intervals dominated by stromatoporoids, corals, and pelmatozoans.

4. Discussion

4.1. Late Aeronian to Sheinwoodian chronostratigraphy of the Midcontinent

This study provides a high-resolution chemostratigraphic framework, bracketed by biostratigraphic tie points, that constrains the age distribution of facies packages in the late Aeronian to basal Sheinwoodian of the midcontinent. Beginning at the base of the studied succession, the negative $\delta^{13}C_{carb}$ interval within the upper Burnt Bluff Formation is a distinct feature within the mid-Llandovery and is regarded as diagnostic of the Aeronian-Telychian stage boundary (Figs. 1 and 4; *sensu* Cramer et al., 2011). The immediately overlying positive excursion within the Schoolcraft Formation contains the conodont *Pseudolonchodina fluegeli* (Kuglitsch, 2000) that coincides with the shift from *Pentamerus* to *Pentameroides* brachiopod genera near the top of the excursion. The distinctive $\delta^{13}C_{carb}$ profile, combined with these biostratigraphic markers, constrains the lower positive $\delta^{13}C_{carb}$ excursion to the lower Telychian Valgu Excursion of Munnecke and Männik (2009). The zonally diagnostic conodont *Kockelella ranuliformis* in the Waukesha Formation in Milwaukee (Kuglitsch, 2000) is coincident with the uppermost positive excursion, demonstrating that it is unmistakably the Ireviken Excursion, the onset of which functionally marks the Telychian-Sheinwoodian boundary globally (Fig. 2; Cramer et al., 2010; Munnecke et al., 2010). Constraint of the middle positive excursion between the lower Telychian Valgu and early Sheinwoodian Ireviken excursions identify this anomaly as a previously unrecognized $\delta^{13}C_{carb}$ excursion. Conodont $^{87}Sr/^{86}Sr$ values of 0.70829 from near the base of this excursion (Fig. 1; Kuglitsch, 2000; Egg Harbor section, ~20 km from the Jarmen Rd. core DO-394) and the striking similarity of the Sheboygan $\delta^{13}C_{carb}$ curve to the biostratigraphically well-constrained Estonian Viki core (Fig. 2) suggest that the age of this positive $\delta^{13}C_{carb}$ excursion is near the conodont *Pt. celloni* Superzone—*Pt. am. amorphognathoides* Zonal Group boundary. We name and define this mid-Telychian feature in the $\delta^{13}C_{carb}$ curve the Manitowoc Excursion.

4.2. Covariation of sequence stratigraphic and $\delta^{13}C_{carb}$ patterns

Analysis of the chronostratigraphically ordered facies succession confirms that the late Aeronian to early Sheinwoodian age strata of the Michigan Basin are divisible into three 3rd-order depositional sequences that show covariance with $\delta^{13}C_{carb}$ patterns (Fig. 7; Brett et al., 1990). The age distribution of these sequences is close to those defined in the Appalachian Basin and, thus, we use that nomenclature here. In the study area, the basal part of Silurian sequence II begins with a maximum flooding interval developed in

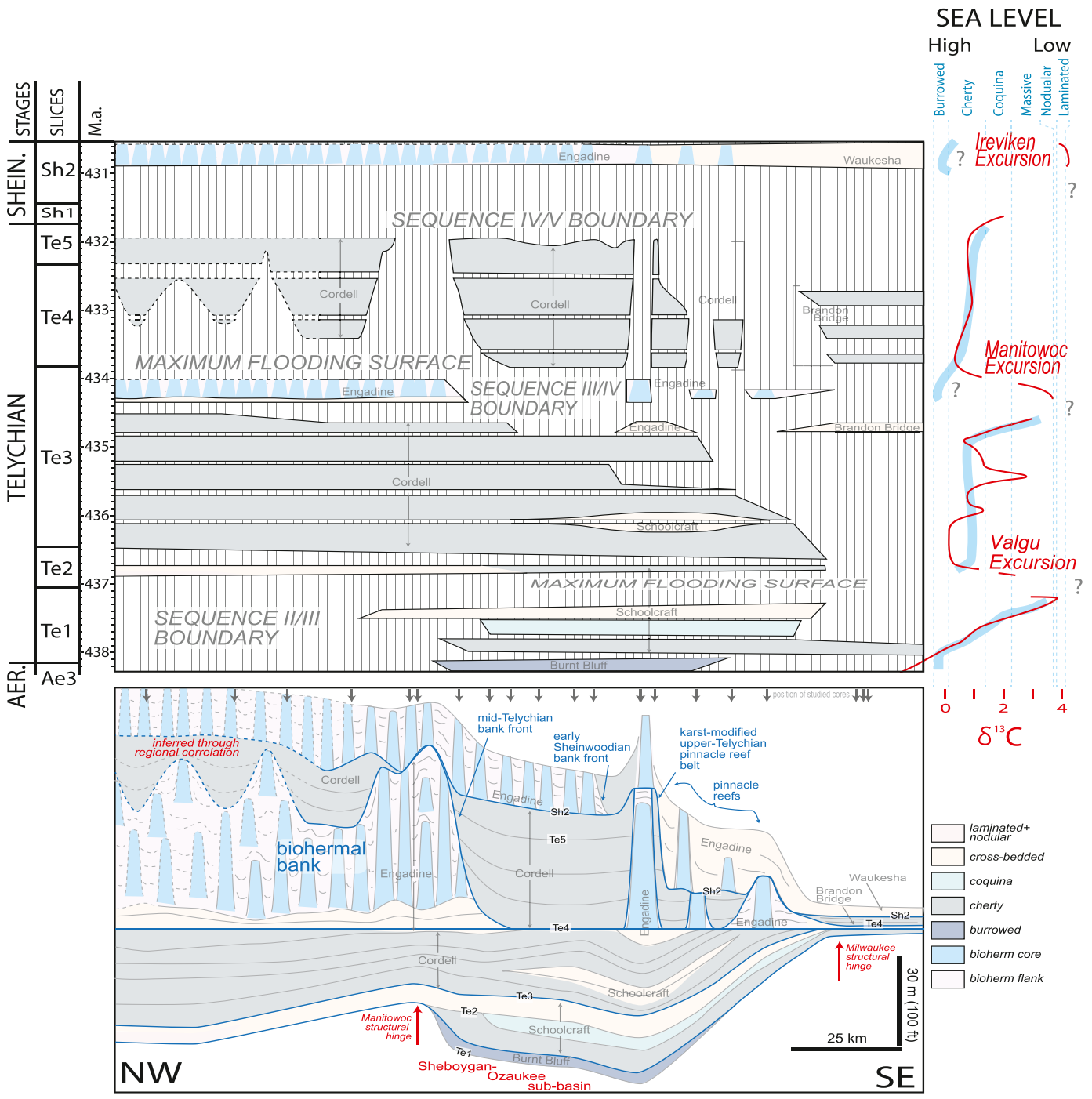

Fig. 7. Interpretive facies cross section derived from relations in Fig. 4 (lower panel, see key for facies color scheme) and inferred chronostratigraphy, sequence stratigraphy, $\delta^{13}C_{carb}$ stratigraphy, and sea level history (upper panel; blue dashed lines indicate facies boundaries). Note the incomplete nature of the $\delta^{13}C_{carb}$ and sea level curves reflects gaps in the record marked by sequence boundaries and maximum flooding surfaces (after those of Brett et al., 1990). SHEIN. = Sheinwoodian, AER. = Aeronian.

the upper Burnt Bluff. Regression is apparent in the progression from burrowed to cherty facies upward into the Schoolcraft, culminating in mud-cracked laminite facies and hardgrounds marking subaerial exposure (Silurian sequence II/III boundary). This regressive facies succession is paralleled by rising values in the ascending limb of the Valgu Excursion (Fig. 7). Sequence III begins with an abrupt deepening, indicated by the shift to cherty facies of the Cordell Formation. Strata of this relatively deep-water facies persist for tens of meters up-section, showing little shallowing or deepening trend. The interval is capped by a cluster of hardgrounds (datum of Fig. 4) and an abrupt shift to the cross-bedded facies of the Engadine Formation. This facies offset is interpreted as the Silurian III-IV sequence boundary (*sensu* Brett et al., 1990), an unconformity widely recognized across the North American midcontinent (cf., Kluessendorf and Mikulic, 1996). This unconformity is directly overlain by strata containing the Manitowoc Excursion. Sequence IV, beginning with cross-bedded facies of the Engadine Formation, transitions upward to reefal facies as much as 50 m thick, marking the transgressive systems tract. In places the reefs are overlain and separated laterally by the cherty facies of the upper tongue of the Cordell Formation of the sequence IV highstand systems tract. The succession is capped by an abrupt reappearance of the cross-bedded and reefal facies (i.e., upper tongue of Engadine Formation) across much of the study area and a positive shift

in $\delta^{13}C_{carb}$ values of up to 3‰. In several sections, this contact is a bored and mineralized hardground representing subaerial exposure and subsequent marine modification, marking the base of sequence V (Telychian-Sheinwoodian boundary; Fig. 4). These new chronostratigraphic constraints on the late Aeronian to early Sheinwoodian age strata of the North American midcontinent reveal a striking relationship between shifting facies patterns, representing changes in sea level and the $\delta^{13}C_{carb}$ profile (Fig. 7). Of particular note, the ascending limbs of the positive $\delta^{13}C_{carb}$ excursions correspond with facies changes consistent with progressive sea level fall. The associated deposits are capped by exposure surfaces at peak $\delta^{13}C_{carb}$ values, which are in turn overlain by reefs. The comparison of this Michigan Basin succession with strata in other parts of Laurentia further reinforces these patterns (Fig. 8).

4.3. Synchroneity with adjacent basins

Despite differences in tectonic history and proximity to the open ocean, the carbonate-dominated Michigan and Anticosti basins have strikingly similar Telychian facies and $\delta^{13}C_{carb}$ trends. On Anticosti, the ascending limb of the Valgu Excursion culminates with crinoidal shoal facies having peak $\delta^{13}C_{carb}$ values (Fig. 8; Munnecke and Männik, 2009). The overlying lower Chicotte Formation contains prominent erosional surfaces (Desrochers, 2006), one of which may mark the subaerial unconformity separating sequences II and III (*sensu* Brett et al., 1990). Above this surface, the occurrence of small 2- to 10-m-thick muddy reef deposits (~15 m above the base of the Chicotte Formation), which lack photic zone indicators, has been interpreted as a substantial transgression (Desrochers et al., 2007). Most striking is an unconformity surface developed on the middle Chicotte (i.e., the "mid-Chicotte unconformity" of James et al., 2015) that is characterized by up to 50 m of relief; we suggest that this is the sequence boundary separating sequences III and IV. Importantly, the minimum amount of relative sea-level fluctuation required to form this unconformity surface and, subsequently, to build pinnacle reefs in the Michigan Basin is at least 50 m.

Sequence stratigraphic patterns preserved within the late Aeronian to early Sheinwoodian strata of the Appalachian Basin (McLaughlin et al., 2012) are also similar to the Michigan Basin succession (Fig. 8). The mixed carbonate-siliciclastic setting of the Appalachian Basin provides valuable additional insight as the clastic sediments accentuate some eustatic patterns. For example, diminished clastic sediment inputs to the basin during transgression generally stimulates carbonate production, whereas the influx of siliciclastic sediment during regression generally suppresses it (cf., Brett et al., 1990; McLaughlin et al., 2012). Within the Appalachian Basin, the rising limbs of the Valgu, Manitowoc, and Ireviken positive $\delta^{13}C_{carb}$ excursions are accompanied by progradation of sand and silt wedges from the clastic margin (Fig. 8). In the case of the Valgu and Manitowoc excursion intervals, the regressive sands are capped by maximum flooding surfaces with iron mineralization and outsized clasts that represent transgressive lag deposits, overlain by offshore shales. On the opposing cratonic margin of the basin, transgressive packages are defined by thin phosphatic and glauconitic carbonate successions. The Ireviken Excursion interval is noteworthy because the regressive sequence is abruptly superseded by a transgressive interval characterized by interbedded ironstones and quartz arenites overlain by offshore shales that developed on the clastic margin associated with a short-lived negative $\delta^{13}C_{carb}$ excursion (>3.0‰), during an otherwise positive excursion interval. On the cratonic margin of the basin, this transitory negative excursion is preserved in the gray shales and thin glauconitic skeletal carbonates that mark the contact with the Rochester Shale. Positive $\delta^{13}C_{carb}$ values return with the sudden appearance of small reefs (0.5–5.0 m tall). This negative excursion has also been recorded in the early part of the Ireviken Excursion using organic carbon isotopes in the Baltic and Welsh basins (reference horizon 2 of Cramer et al., 2010), which reflects its global nature. This prominent but short-lived event has yet to be directly documented in the carbonate-dominated succession of the Michigan Basin (Fig. 7).

Prior to interpreting the processes that generated the $\delta^{13}C_{carb}$ patterns recognized above, it is critical that they are evaluated through standard tests. Isotopic studies of carbonates deposited in modern restricted shallow marine environments show that the interpretation of $\delta^{13}C_{carb}$ profiles should be approached with caution (Supplemental Text Section 1). Specifically, these studies show that carbon in modern shallow marine environments can be isotopically decoupled from the open ocean dissolved inorganic carbon (DIC) reservoir and that global sea level fluctuations can cause synchronous changes in $\delta^{13}C_{carb}$ of platform sediments that are unrelated to the global carbon cycle. Integration of high-resolution $\delta^{13}C_{carb}$ stratigraphy, sedimentology, sequence- and chrono-stratigraphic correlation within the Michigan and adjacent basins indicate pinnacle reef growth and a host of paleoenvironmental changes might be tied to the global carbon cycle. In light of the potential import of these relationships, we combined the results of our study, a robust literature review, and established methodologies from studies of modern and ancient carbonate depositional environments to thoroughly evaluate the fidelity of our results as viable proxy records of the global carbon cycle (Supplemental Text Section 1). Together, our holistic integration of these data and observations, possibly the richest for any Paleozoic event, indicates by all measures that these phenomena are linked to perturbations of the global carbon cycle.

4.4. A sea level paradox

Facies analysis of rocks preserved in the Michigan, Appalachian, and Anticosti basins define a consistent relationship between Llandovery-Wenlock sequence stratigraphic and $\delta^{13}C_{carb}$ trends. As emphasized previously, the rising limbs of these positive $\delta^{13}C_{carb}$ excursions are accompanied by synchronized shallowing trends that culminate in subaerial exposure surfaces at peak $\delta^{13}C_{carb}$ values (Fig. 8). Notably, strata deposited during the Wenlock and Ludlow age Mulde and Lau positive $\delta^{13}C_{carb}$ excursions, respectively, preserve similar patterns (Calner, 2006). Further, the observed shallowing is consistent with $\delta^{18}O$ data that link distinct cooling events with the positive $\delta^{13}C_{carb}$ excursions (Fig. 1; Trotter et al., 2016). Paradoxically, the subaerial exposure surfaces are overlain by pinnacle reef successions that retain the peak values of the $\delta^{13}C_{carb}$ excursion. These patterns are not unique to this interval; in fact, they closely match classic carbonate depositional models in which pinnacle reefs rest on hardgrounds outboard of the shelf margin or on the steepened distal margins of ramps (cf., Kendal and Schlager, 1981). Silurian pinnacle reefs above the exposure surfaces have "catch up" geometries suggesting growth during transgression to early highstand in relatively deep water (Sarg, 1988).

The observation that these reefs nucleate on or just above exposure surfaces, but still record peak $\delta^{13}C_{carb}$ values, when sea level should be at its lowest, raises an important question—why does sea level suddenly appear to decouple from the global carbon cycle? Likely, normal subsidence rates within this intracratonic basin (~1 m per 70 k.y.; Figs. 4 and 7) are inadequate to produce requisite water depths because the duration of Silurian carbon isotope excursions is generally <1.0 m.y. (e.g., Cramer et al., 2012). Similarly, rapid tectonic subsidence events are an unlikely mechanism because they would have to correlate precisely with multiple global carbon cycle events that occurred synchronously across multiple basins and continents. Unfortunately, the stratigraphic

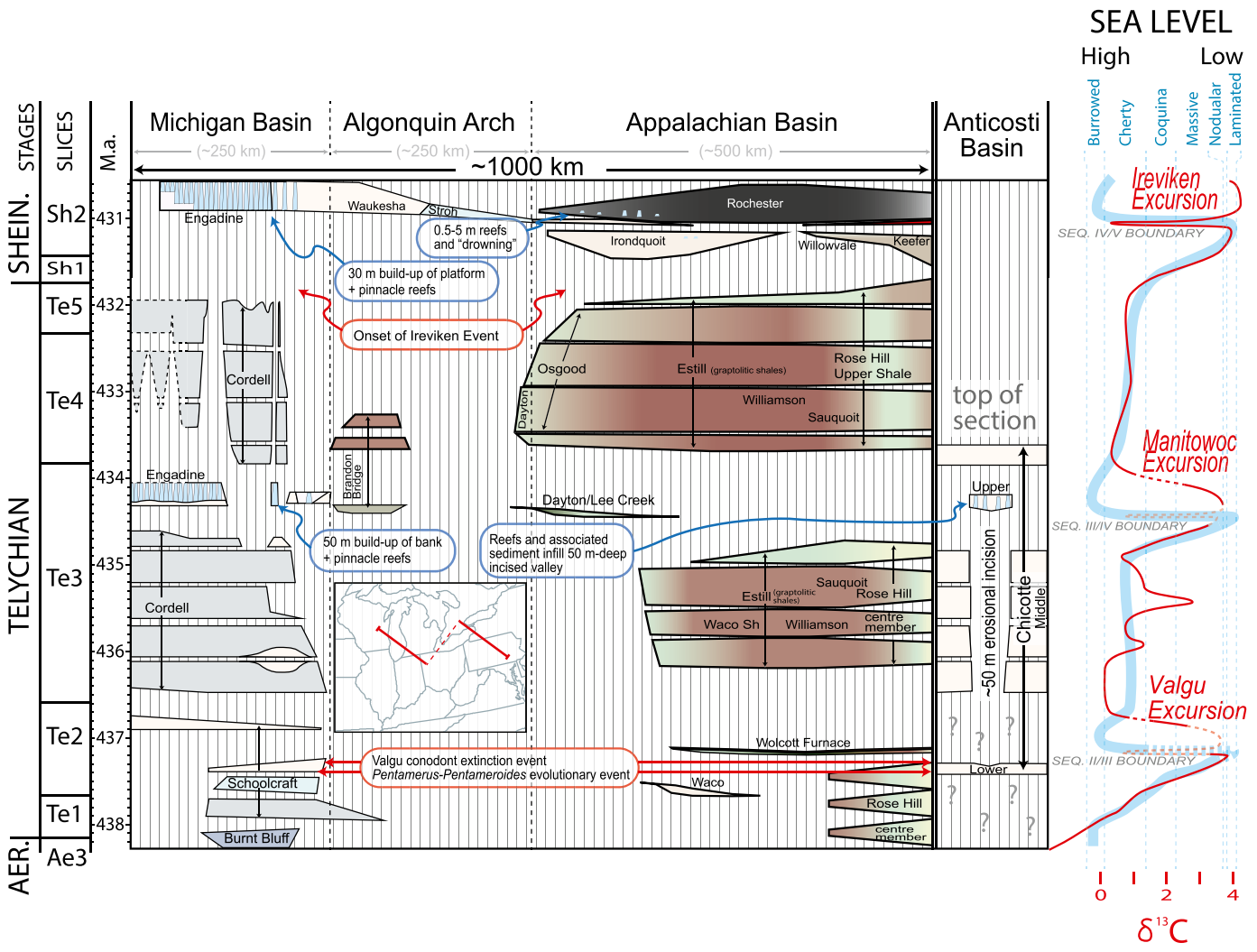

Fig. 8. Chronostratigraphic correlation across southern Laurentia and the timing of events. Michigan Basin data from Fig. 7; Appalachian Basin chronostratigraphy modified from McLaughlin et al. (2012); and Anticosti Basin chronostratigraphy and facies interpretations modified from Desrochers et al. (2007) and James et al. (2015). Note the completed sea level and $\delta^{13}C_{carb}$ patterns for the Ireviken Excursion interval and those inferred (dashed lines) through recognition of similar patterns for the Manitowoc and Valgu excursion intervals. Position of bio-events noted by red outlined ovals and features associated with reef episodes noted in blue outline.

record of exposure and flooding is incomplete in the Michigan Basin (condensed into one or a cluster of closely spaced hardgrounds), which enhances the importance of the relatively complete Ireviken Excursion record in the mixed carbonate-siliciclastic setting of the Appalachian Basin. Specifically, the transitory >3.0‰ negative excursion in the early part of the Ireviken positive excursion coincides with the sudden basin flooding recorded in the first appearance of the Rochester Shale (McLaughlin et al., 2012). This record indicates deep-water facies persisted through the rebound to peak $\delta^{13}C_{carb}$ values and are accompanied by the growth of 1- to 5-m-tall bioherms just above the negative excursion. The magnitude and short duration of the sharp decrease in $\delta^{13}C_{carb}$ values suggest a sudden injection of light carbon from methane, as has been increasingly observed in the geologic record (cf., Kump et al., 2009). Injecting a greenhouse gas more than two orders of magnitude more powerful than CO_2 would have caused a fleeting pulse of warming (because methane decays rapidly in the atmosphere). Such a brief pulse might have yielded short-lived but dramatic sea level rise similar to other negative excursions, superimposed on otherwise positive excursion events. Although an in-depth analysis is beyond the scope of this study, the similarity of the Valgu and Manitowoc excursion records to the Ireviken raises the tantalizing prospect that transient releases of methane may be an intrinsic component of these global carbon cycle perturbations in the Silurian. If so, fleeting and rarely identified methane releases may be the underlying culprit responsible for decoupling sea level and carbon isotope records during positive $\delta^{13}C_{carb}$ excursions. Moreover, the sudden occurrence of reefs across the Appalachian and Michigan basins during recovery to peak $\delta^{13}C_{carb}$ values may accord with the concept of "calcification overshoot" that drives hypercalcification immediately following acidification events (Kump et al., 2009). The idea that the effects of ephemeral methane release (marked by short-lived negative $\delta^{13}C_{carb}$ excursions) during otherwise positive excursions may be concealed in these fragmented stratigraphic records is highly speculative, but warrants further investigation, because these secondary processes might ultimately refine our understanding of the origin of pinnacle reefs.

4.5. The evolution of pinnacle reefs

Viewed at high chronostratigraphic resolution (<1 m.y.), periods of Silurian reef growth and evolution are strongly correlated with positive $\delta^{13}C_{carb}$ excursions, which therefore constitute important temporal datums. The first two pinnacle reef tracts recorded in the geologic record correspond precisely with the Silurian Manitowoc (mid-Telychian) and Ireviken (early Sheinwoodian) excursions in the North American midcontinent. Revolutionary

advances in global stratigraphic correlation provided by integrated bio- and chemostratigraphy demonstrate that these evolutionary reef episodes are traceable across Laurentia and to other regions globally. The remarkable synchroneity between $\delta^{13}C_{carb}$ isotope excursions and reef proliferation events (Figs. 2 and 9), also noted in younger Silurian intervals (Calner, 2006), suggests reef evolution and $\delta^{13}C_{carb}$ excursions are mechanistically linked.

In light of the prominent correlation between Silurian reef proliferation and $\delta^{13}C_{carb}$, we examined the upper Cambrian through Lower Devonian stratigraphic record for similar patterns using the ever-increasing availability of published $\delta^{13}C_{carb}$ profiles (Supplemental Data Table 3 for references). Extensive compilations pertinent to reef distribution in time and space and $\delta^{13}C_{carb}$ stratigraphy define a striking relationship between previously identified "reef episodes," separated by longer periods of muted reef growth, and $\delta^{13}C_{carb}$ excursions (Fig. 9). Individual examples of this wide-ranging relationship were previously identified for some intervals. As mentioned in the Introduction, the late Cambrian SPICE event is characterized by a global +4.0 to +6.0‰ $\delta^{13}C_{carb}$ excursion. In an extensive review of calcic organisms through this interval, Lee et al. (2015) noted the correspondence between several geologic/biologic phenomena and positive carbon isotope excursions. Specifically, they note the coincidence of eustatic sea level fall, major faunal turnover, and a shift from thrombolites and dendrolites to sponge-microbial associations of maze-like reefs and columnar stromatolites. A proliferation of sponges and stromatolites dominated reefs upon the subsequent sea level rise (still within the $\delta^{13}C_{carb}$ excursion), interpreted as a resurgence of new reef-building metazoans after the decline of archaeocyaths at the end of Cambrian Epoch 2. While the relationship between abundant Lower Ordovician microbial reefs and associated $\delta^{13}C_{carb}$ excursions is not exact, a broader pattern seems reasonably well established. The metazoan colonization/diversification of reefs during the prolonged Great Ordovician Biodiversification Event (GOBE) contains the middle Darriwilian $\delta^{13}C_{carb}$ excursion (MDICE). In Laurentia, strata displaying the MDICE (Edwards and Saltzman, 2016) are considered lateral equivalents of enigmatic localized pinnacle reef occurrences that did not form a distinctive reef tract. Characterized by relatively small reefs, an early Katian reef episode in Baltica occurred during the Guttenberg Excursion (GICE; Kroger et al., 2016). Reefs are generally missing through much of the remaining Katian. Perhaps the very first small pinnacle reef tract occurs over ~300 km in a portion of the Baltic Basin in the latest Katian during the Paroveja Excursion. Enigmatically, during the Hirnantian Excursion (HICE), despite glacioeustastatic oscillation rivaling the Pleistocene, reefs are relatively few in number and small in stature, achieving little more than a few meters of synoptic relief (Copper, 2001). With the exception of a few rare pinnacle reefs at the base of the Silurian, the Rhuddanian, Aeronian, and early Telychian reefs are also small, scattered, and episodic (Copper, 2002). During the mid-Telychian, development of the pinnacle reef tract associated with the Manitowoc Excursion appears to represent a fundamental shift in the morphology, abundance, and size of reefs. Subsequent $\delta^{13}C_{carb}$ excursions (Fig. 9) are characterized by the synchronous proliferation of pinnacle reef tracts across the paleo-tropics during the middle to upper Silurian (Calner, 2006) and into the Devonian (Bourque et al., 1986).

While the combined geologic and biologic evidence for reef episodes through the lower Paleozoic appears to be strongly correlated with global carbon cycle perturbations, important questions remain. For example, what processes mediated the sudden evolutionary change that fostered rapid vertical reef development, resulting in pinnacle reef morphologies? The degree to which short-duration events, such as methane pulses, may be critical and inherent components of the ocean-atmosphere system responsible for pinnacle reef growth merits further investigation. As the stratigraphic records for these critical time intervals are fragmented in carbonate depositional settings, more complete records in mixed carbonate-siliciclastic systems, such as the Appalachian Basin, provide enticing venues for future study.

5. Conclusions

Combined high-resolution carbon isotope stratigraphy and published biostratigraphy allow refinements of the chronostratigraphic framework pertinent to late Aeronian to early Sheinwoodian strata of the Michigan Basin, providing new insights into the origin of pinnacle reefs and their relationship to Silurian carbon cycle perturbations. This framework facilitates stratigraphic correlation at unprecedented temporal resolution, identifies gaps in the succession even in complicated reef intervals, and enables correlation with deposits in the adjoining Anticosti and Appalachian basins. This study constrains the age of the first appearance of Silurian pinnacle reef tracts to the newly recognized mid-Telychian Manitowoc positive $\delta^{13}C_{carb}$ excursion.

High-resolution facies analysis within this temporal framework reveals synchroneity between global $\delta^{13}C_{carb}$ excursions, eustatic sea level trends, and reef growth. Accordingly, variations among these phenomena are likely linked through environmental forcing induced by perturbations of the global carbon cycle. The positive shift of $\delta^{13}C_{carb}$ values corresponds to eustatic shallowing that culminates in exposure surfaces, enigmatically followed by periods of rapid pinnacle reef growth. While the stratigraphic record at the peak of these dynamic events is often incomplete, we have identified tantalizing evidence that the rapid rise in sea level was facilitated by transient releases of methane responsible for warming pulses where initial acidification resulting in carbonate destruction was followed by hypercalcification and pinnacle reef formation.

The coincidence of reef episodes and $\delta^{13}C_{carb}$ excursions spans much of the upper Cambrian through Lower Devonian. Within this longer perspective, the mid-Telychian appearance of pinnacle reef tracts constitutes a distinct event. Consequently, these relationships suggest that the occurrence of early Paleozoic reefs, and correspondingly, the diversification of associate marine organisms that profoundly shaped the trajectory of Earth's evolution, were inextricably linked to the global carbon cycle.

Acknowledgements

We are grateful to Greg Cane at the W. M. Keck Paleoenvironmental and Environmental Stable Isotope Lab at the University of Kansas and Kim Sparks at the Cornell University Stable Isotope Lab for ensuring the highest quality $\delta^{13}C_{carb}$ results. Thanks also to Don Mikulic, Mark Harris, and John Luczaj for discussions of Wisconsin geology and access to cores held at the Illinois State Geological Survey, University of Milwaukee, and University of Wisconsin-Green Bay during the initial stages of this study. The project also benefited from discussions with Matt Rine, Frank Brunton, Nick Sullivan, Brad Cramer, Mark Kleffner, Edward A. du Bray, Charles H. Thorman, and James Thomka. The manuscript benefited greatly from reviews by Steve Kershaw, Jeong-Hyun Lee, and an anonymous reviewer and guidance by Editor Derek Vance. This research was funded in part by the USGS National Cooperative Geological Mapping Program under StateMap awards to the Wisconsin Geological and Natural History Survey from 2010 to 2015 and the Indiana Geological and Water Survey from 2015 to 2018. Additional funding came from NSF EAR 0518511, and the U.S. Geological Survey "CHRONOMAP" project. This paper is a contribution to the International Geoscience Programme (IGCP) 591: The Early to Middle Paleozoic Revolution. Any use of trade, product, or firm names

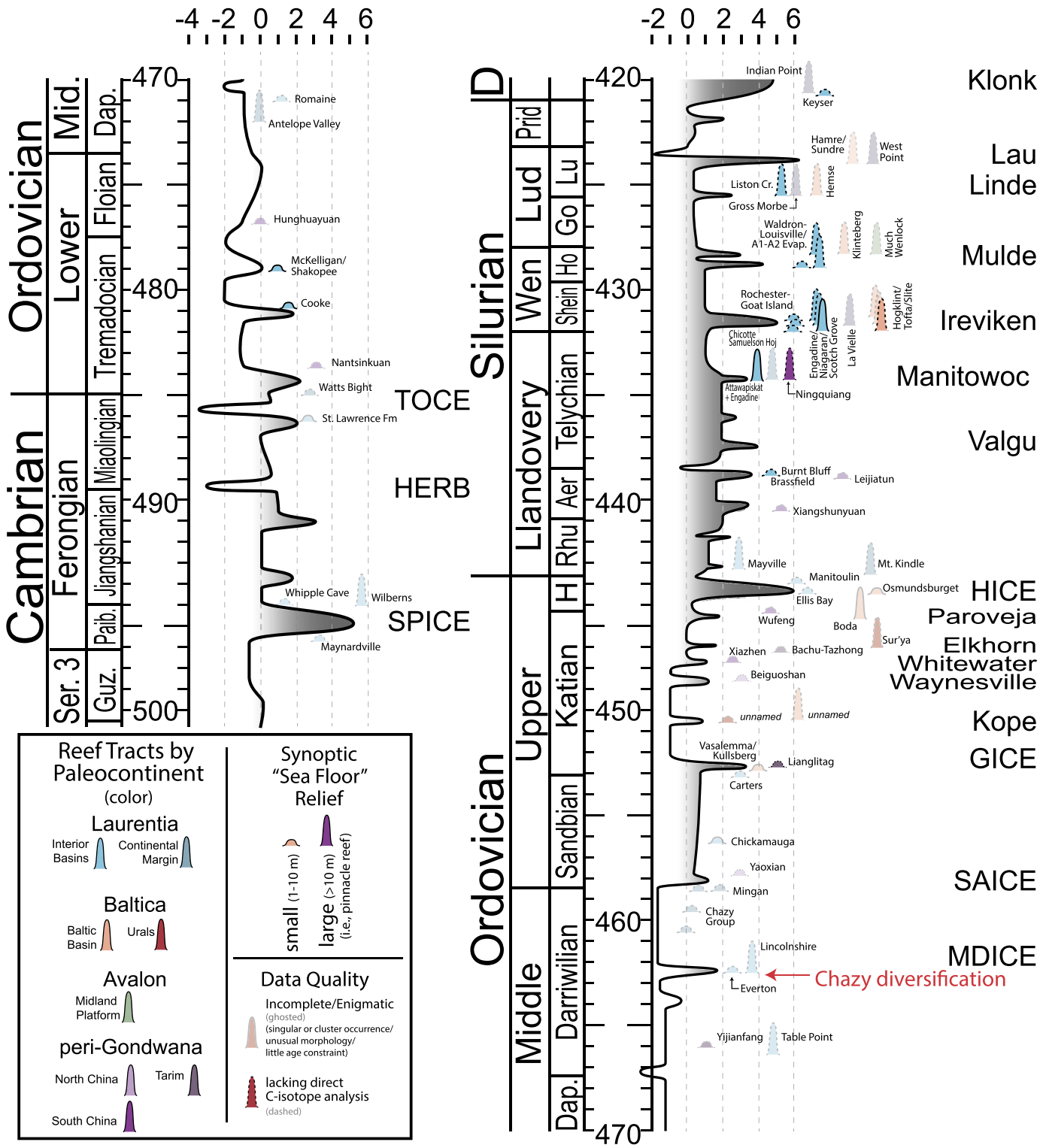

Fig. 9. Distribution of early to middle Paleozoic reefs/reef episodes relative to a generalized $\delta^{13}C_{carb}$ record for the paleocontinents/terranes of Laurentia, Baltica, Avalon, and peri-Gondwana (see Table 2 for references). Base of reef symbol relative to time scale indicates interpreted age.

is for descriptive purposes only and does not imply endorsement by the U.S. Government.

Appendix A. Supplementary material

Supplementary material related to this article can be found online at https://doi.org/10.1016/j.epsl.2019.02.039.

References

Bourque, P.-A., Amyot, G., Desrochers, A., Gignac, H., Gosselin, C., Lachambre, G., Laliberté, J.-Y., 1986. Silurian and Lower Devonian reef and carbonate complexes of the Gaspé Basin, Quebec—a summary. Bull. Can. Pet. Geol. 34, 452–489.

Brett, C.E., Goodman, W.M., LoDuca, S.T., 1990. Sequences, cycles, and basin dynamics in the Silurian of the Appalachian Foreland Basin. Sediment. Geol. 69, 191–244.

Brett, C.E., McLaughlin, P.I., Histon, K., Schindler, E., Ferretti, A., 2012. Time-specific aspects of facies: state of the art, examples, and possible causes. Palaeogeogr. Palaeoclimatol. Palaeoecol. 367–368, 6–18.

Brunton, F.R., Smith Dixon, O.A., Copper, P., Nestor, H., Kershaw, S., 1998. Silurian reef episodes, changing seascapes and paleobiogeography. In: Brett, C.E., Baird, G. (Eds.), The James Hall Symposium: 2nd International Symposium on the Silurian System. In: New York State Bulletin, vol. 491, pp. 259–276.

Calner, M., 2006. Silurian carbonate platforms and extinction events—ecosystem changes exemplified from Gotland, Sweden. Facies 51, 584–591.

Colville, V.R., Johnson, M.E., 1982. Correlation of sea-level curves for the Lower Silurian of the Bruce Peninsula and Lake Timiskaming District (Ontario). Can. J. Earth Sci. 19, 962–974.

Copper, P., 2001. Reefs during the multiple crises towards the Ordovician-Silurian boundary: Anticosti Island, eastern Canada, and worldwide. Can. J. Earth Sci. 38, 153–171.

Copper, P., 2002. Silurian and Devonian reefs: 80 million years of global greenhouse between two ice ages. In: Kiessling, W., Flügel, E., Golonka, J. (Eds.), Phanerozoic Reef Patterns. In: SEPM Special Publication, vol. 72, pp. 181–238.

Cramer, B.D., Loydell, D.K., Samtleben, C., Munnecke, A., Kaljo, D., Mannik, P., Martma, T., Jeppson, L., Kleffner, M.A., Barrick, J.E., Johnson, C.A., Emsbo, P., Joachimski, M.M., Bickert, T., Saltzman, M.R., 2010. Testing the limits of Paleozoic chronostratigraphic correlation via high-resolution (<500 k.y.) integrated conodont, graptolite, and carbon isotope ($\delta^{13}C_{carb}$) biochemostratigraphy across the Llandovery-Wenlock (Silurian) boundary: is a unified Phanerozoic time scale achievable. Geol. Soc. Am. Bull. 122, 1700–1716.

Cramer, B.D., Brett, C.E., Melchin, M.J., Männik, P., Kleffner, M.A., McLaughlin, P.I., Loydell, D.K., Munnecke, A., Jeppsson, L., Corradini, C., Brunton, F.R., Saltzman, M.R., 2011. Revised correlation of the Silurian Provincial Series of North America with global and regional chronostratigraphic units and $\delta^{13}C_{carb}$ chemostratigraphy. Lethaia 44, 185–202.

Cramer, B.D., Condon, D.J., Soderlund, U., Marshall, C., Worton, G.J., Thomas, A.T., Calner, M., Ray, D.C., Perrier, V., Boomer, I., Patchett, J., Jeppsson, L., 2012. U–Pb (zircon) age constraints on the timing and duration of Wenlock (Silurian) paleocommunity collapse and recovery during the "Big Crisis". Geol. Soc. Am. Bull. 124, 1841–1857.

Desrochers, A., 2006. Rocky shoreline deposits in the Lower Silurian (upper Llandovery, Telychian) Chicotte Formation, Anticosti Island, Quebec. Can. J. Earth Sci. 43, 1205–1214.

Desrochers, A., Bourque, P., Neuweiler, F., 2007. Diagenetic versus biotic accretionary mechanisms of bryozoan-sponge buildups (lower Silurian, Anticosti Island, Canada). J. Sediment. Res. 77, 564–571.

Edwards, C.T., Saltzman, M.R., 2016. Paired carbon isotopic analysis of Ordovician bulk carbonate ($\delta^{13}C_{carb}$) and organic matter ($\delta^{13}C_{org}$) spanning the Great Ordovician Biodiversification Event. Palaeogeogr. Palaeoclimatol. Palaeoecol. 458, 102–117.

Emsbo, P., 2017. Sedex brine expulsions to Paleozoic basins may have changed global marine $^{87}Sr/^{86}Sr$ values, triggered anoxia, and initiated mass extinctions. Ore Geol. Rev. 86, 474–486.

Flügel, E., Kiessling, W., 2002. A new look at ancient reefs. In: Kiessling, W., Flügel, E., Golonka, J. (Eds.), Phanerozoic Reef Patterns. In: SEPM Special Publication, vol. 72, pp. 735–743.

Gill, B.C., Lyons, T.W., Young, S.A., Kump, L.R., Knoll, A.H., Saltzman, M.R., 2011. Geochemical evidence for widespread euxinia in the Later Cambrian ocean. Nature 469, 80–83.

Harris, M.T., Waldhuetter, K.R., 1996. Silurian of the Great Lakes region, part 3: Llandovery strata of the Door Peninsula, Wisconsin. Milwaukee Public Museum Contrib. Biol. Geol. 90. 162 p.

Heckel, P.H., 1974. Carbonate buildups in the geologic record: a review. In: Laporte, L.F. (Ed.), Reefs in Time and Space. In: Society for Sedimentary Geology (SEPM) Special Publication, vol. 18, pp. 90–154.

James, N.P., Wood, R.A., 2010. Reefs. In: James, N.P., Dalrymple, R.W. (Eds.), Facies Models: Response to Sea Level Change. Geological Association of Canada, pp. 421–447.

James, N.P., Desrochers, A., Kyser, K., 2015. Polygenic (polyphase) karsted hardground omission surfaces in lower Silurian neritic limestones: Anticosti Island, eastern Canada. J. Sediment. Res. 85, 1138–1154.

Jenkyns, H.C., Gale, A.S., Corfield, R.M., 1994. Carbon- and oxygen-isotope stratigraphy of the English Chalk and Italian Scaglia and its palaeoclimatic significance. Geol. Mag. 131, 1–34.

Johnson, M.E., Colville, V.R., 1982. Regional integration of evidence for evolution in the Silurian *Pentamerus-Pentameroides* lineage. Lethaia 15, 41–54.

Kaljo, D., Kiipli, T., Martma, T., 1997. Carbon isotope event markers through the Wenlock-Pridoli sequence at Ohesaare (Estonia) and Priekule (Latvia). Palaeogeogr. Palaeoclimatol. Palaeoecol. 132, 211–223.

Kaljo, D., Martma, T., Mannik, P., Viira, V., 2003. Implications of Gondwana glaciations in the Baltic late Ordovician and Silurian and a carbon isotopic test of environmental cyclicity. Bull. Soc. Géol. Fr. 174, 59–66.

Kendal, C.G.St.C., Schlager, W., 1981. Carbonates and relative changes in sea level. Mar. Geol. 44, 181–212.

Kiessling, W., 2002. Secular variations in the Phanerozoic reef ecosystem. In: Kiessling, W., Fluegel, E., Golonka, J. (Eds.), Phanerozoic Reef Patterns. In: SEPM Special Publication, vol. 72, pp. 625–690.

Kiessling, W., Flügel, E., Golonka, J., 2003. Patterns of Phanerozoic carbonate platform sedimentation. Lethaia 36, 195–255.

Kiessling, W., Simpson, C., Foote, M., 2010. Reefs as cradles of evolution and sources of biodiversity in the Phanerozoic. Science 327, 196–198.

Kleffner, M.A., Norby, R.D., Kluessendorf, J., Mikulic, D.G., 2018. Revised conodont biostratigraphy of lower Silurian strata of southwestern Wisconsin. Abstr. Program – Geol. Soc. Am. 50. https://doi.org/10.1130/abs/2018NC-312921.

Kluessendorf, J., Mikulic, D.G., 1996. An early Silurian sequence boundary in Illinois and Wisconsin. In: Witzke, B.J., Ludvigson, G.A., Day, J. (Eds.), Paleozoic Sequence Stratigraphy: Views from the North American Craton. In: Spec. Pap., Geol. Soc. Am., vol. 306, pp. 177–185.

Kroger, B., Hints, L., Lehnert, O., 2016. Ordovician reef and mound evolution: the Baltoscandian picture. Geol. Mag. 154, 683–706.

Kuglitsch, J.J., 2000. Correlation of the Silurian Rocks of Southeastern and Northeastern Wisconsin Using Conodonts and Conodont Strontium Isotope Ratios and Proposed Conodont and Ostracode Biofacies Models for the Environs of the Middle Aeronian Michigan Basin. Ph.D. dissertation. University of Wisconsin–Madison. 349 p.

Kump, L.R., Bralower, T.J., Ridgwell, A., 2009. Ocean acidification in deep time. Oceanography 22, 94–107.

Lee, J., Chen, J., Chough, S.K., 2015. The middle-late Cambrian reef transition and related geological events: a review and new view. Earth-Sci. Rev. 145, 66–84.

McLaughlin, P.I., Emsbo, P., Brett, C.E., 2012. Beyond black shales: the sedimentary and stable isotope records of oceanic anoxic events in a dominantly oxic basin (Silurian; Appalachian Basin, USA). Palaeogeogr. Palaeoclimatol. Palaeoecol. 367–368, 153–177.

McLaughlin, P.I., Mikulic, D., Kluessendorf, J., 2013. Age of Silurian rocks in Sheboygan County Wisconsin from stable carbon isotope analysis. Geosci. Wisconsin 21, 15–38.

Mikulic, D.G., Kluessendorf, J., 1998. Sequence stratigraphy and depositional environments of the Silurian and Devonian rocks of southeastern Wisconsin. In: Guidebook for the 1998 Fall Field Conference for the Joint Meeting of SEPM Great Lakes Section and The Michigan Basin Geological Society. 84 p.

Munnecke, A., Männik, P., 2009. New biostratigraphic and chemostratigraphic data from the Chicotte Formation (Llandovery, Anticosti Island, Laurentia) compared with the Viki core (Estonia, Baltica). Est. J. Earth Sci. 58, 159–169.

Munnecke, A., Calner, M., Harper, D.A.T., Servais, T., 2010. Ordovician and Silurian sea-water chemistry, sea level, and climate: a synopsis. Palaeogeogr. Palaeoclimatol. Palaeoecol. 296, 389–413.

Rexroad, C., 1980. Stratigraphy and conodont paleontology of the Cataract Formation and the Salamonie Dolomite (Silurian) in northeastern Indiana. Indiana Geol. Surv. Bull. 58. 83 pp.

Riding, R., 2006. Microbial carbonate abundance compared with fluctuations in metazoan diversity over geological time. Sediment. Geol. 185, 229–238.

Riding, R., 2011. Microbialites, stromatolites, and thrombolites. In: Reitner, J., Thiel, V. (Eds.), Encyclopedia of Geobiology, pp. 635–654.

Runkel, A.C., McKay, R.M., Palmer, A.R., 1998. Origin of a classic cratonic sheet sandstone: stratigraphy across the Sauk II-Sauk III boundary in the Upper Mississippi Valley. Geol. Soc. Am. Bull. 110, 188–210.

Sarg, R., 1988. Carbonate sequence stratigraphy. In: Wilgus, C.K., Hastings, B.S., Posamentier, H., Wagoner, J., Ross, C.A., Kendall, C.G.St.C. (Eds.), Sea-Level Changes: An Integrated Approach. In: SEPM Special Publication, vol. 42, pp. 155–181.

Schlager, W., 2005. Carbonate Sedimentology and Sequence Stratigraphy. SEPM Concepts in Sedimentology and Paleontology, vol. 8. 199 pp.

Sønderholm, M., Harland, T.L., 1989. Franklinian reef belt, Silurian, north Greenland. In: Geldsetzer, H.H.J., James, N.P., Tebbutt, G.E. (Eds.), Reefs, Canada and Adjacent Area. In: Mem. - Can. Soc. Pet. Geol., vol. 13, pp. 356–366.

Trotter, J.A., Williams, I.S., Barnes, C.R., Männik, P., Simpson, A., 2016. New $\delta^{18}O$ records of Silurian climate change: implications for environmental and biological events. Palaeogeogr. Palaeoclimatol. Palaeoecol. 443, 34–48.

Waid, C.B., Cramer, B.D., 2017. Global chronostratigraphic correlation of the Llandovery Series (Silurian System) in Iowa, USA, using high-resolution carbon isotope ($\delta^{13}C_{carb}$) chemostratigraphic and brachiopod biostratigraphy. Bull. Geosci. 92, 373–390.

Watkins, R., McGee, P.E., 1994. Silurian of the Great Lakes region, part 2: paleontology of the upper Llandovery Brandon Bridge Formation, Walworth County, Wisconsin. Milwaukee Public Museum Contrib. Biol. Geol. 87. 71 pp.

Webby, B., 2002. Patterns of Ordovician reef development. In: Kiessling, W., Flügel, E., Golonka, J. (Eds.), Phanerozoic Reef Patterns. In: SEPM Special Publication, vol. 72, pp. 129–179.